

Cu₂Cu₂SOD are the result of an imidazolate bridge-splitting process. The fact that the thiocyanate adduct of Cu₂Cu₂SOD remains catalytically active as a superoxide dismutase implies that the bridge is not essential for the enzyme mechanism.² The compound [Cu₂(SCN)₄CA'] is the latest member of a rapidly growing class of bimetallic complexes of binucleating macrocycles.²⁶ Further bioinorganic and organometallic studies of this new area of coordination chemistry will be of interest.

(26) (a) "Copper Coordination Chemistry: Biochemical and Inorganic Perspectives"; Karlin, K. D., Zubieta, J., Eds.; Adenine Press: New York, 1983; Martin, A. E., Lippard, S. J., p 395. (b) Nelson, S. M., p 331. (c) Agnus, Y. L., p 371. (d) Bulkowski, J. E., Summers, W. E., III, p 445. (e) Comarmond, J., Plumerè, P.; Lehn, J.-M.; Agnus, Y.; Louis, R.; Weiss, R.; Kahn, O.; Morgenstern-Badarau, I. *J. Am. Chem. Soc.* **1982**, *104*, 6330.

Acknowledgment. This work was supported by grants from the National Institute of General Medical Sciences (NIGMS), NIH, and the National Science Foundation. A.E.M. was the recipient of a National Research Service Award, GM 07956, from the NIGMS. We thank Mr. Joel Wirth for experimental assistance and Dr. L. S. Hollis for help with the crystallography.

Registry No. 1(ClO₄)₃, 76096-70-3; 2, 89302-54-5; 3, 89302-56-7; Cu₂Cu₂SOD, 9054-89-1.

Supplementary Material Available: Tables S1-S3 listing hydrogen atom positional parameters, thermal parameters for all the atoms, and observed and calculated structure factors for **2** (19 pages). Ordering information is given on any current masthead page.

Binuclear Molybdenum Carbonyls Bridged Both by Hydride and by Bidentate Phosphine Ligands. Crystal and Molecular Structures of Salts of (μ-H)(μ-Ph₂P(CH₂)_nPPh₂)Mo₂(CO)₈⁻ (n = 1-4) and Their Reactions with Acids

Marcetta Y. Darensbourg,*^{1a} Ramadan El Mehdawi,^{1b} Terry J. Delord,^{1c} Frank R. Fronczek,^{1c} and Steven F. Watkins^{1c}

Contribution from the Departments of Chemistry, Texas A&M University, College Station, Texas 77843, Tulane University, New Orleans, Louisiana 70118, and Louisiana State University, Baton Rouge, Louisiana 70803. Received July 12, 1983

Abstract: Reaction of Et₄N⁺ and Ph₄P⁺ salts of μ-HMo₂(CO)₁₀⁻ with bidentate phosphine ligands in refluxing THF yielded salts of μ-HMo₂(CO)₈(Ph₂P(CH₂)_nPPh₂)⁻, n = 1-4, designated as anions **1**⁻, **2**⁻, **3**⁻, and **4**⁻. X-ray crystal structure analyses for two of the new compounds were carried out, and the following parameters were obtained. Ph₄P⁺**1**⁻: P2₁/c, Z = 4, a = 13.886 (6) Å, b = 18.545 (9) Å, c = 20.156 (6) Å, β = 91.03 (4)°, V = 5190 (4) Å³, R = 0.0413 for 4402 reflections with |F_o| ≥ 3σ|F_o|. Et₄N⁺**4**⁻: P1, Z = 2, a = 8.760 (2) Å, b = 13.940 (4) Å, c = 19.686 (4) Å, α = 105.75 (2)°, β = 93.59 (2)°, γ = 97.38 (2)°, V = 2282 (1) Å³, R = 0.0471 for 4720 reflections with |F_o| ≥ 3σ|F_o|. Anions **1**⁻ and **4**⁻ are bridged by both H⁻ and the bidentate ligands and show overall bent, staggered configurations with P₁-Mo₁-Mo₂-P₂ torsion angles of 21° for **1**⁻ and 42° for **4**⁻. Similar framework bends (the intersection angle of (OC)_{ax}-Mo vectors) of ca. 160° and similar Mo₁-H-Mo₂ angles of ca. 131° are observed for **1**⁻ and **4**⁻. The Mo...Mo separation in **1**⁻ is 3.4028 (8) Å and in **4**⁻ it is 3.4995 (8) Å. The distance between the P-donor atoms in **1**⁻ is 3.19 Å and in **4**⁻ it is 5.08 Å. In **4**⁻ the hydride bridge is directed into the area underneath the ligand bridge (the (CH₂)₄ unit), whereas in **1**⁻ the plane of the hydride bridge is roughly perpendicular to the P-CH₂-P bridge. The observed ligand substitution site selection was rationalized on the basis of the best match of bridge ligand donor site separation and intermetal ligand coordination site separation in the bent, staggered form of the parent μ-HMo₂(CO)₁₀⁻. A specific synthesis of the dibridged neutral bimetallics (μ-Ph₂P(CH₂)_nPPh₂)(μ-Ph₂P(CH₂)₂PPh₂)Mo₂(CO)₈ (n = 1, 2) and (μ-Ph₂As(CH₂)₂AsPPh₂)(μ-Ph₂P(CH₂)₂PPh₂)Mo₂(CO)₈ has been based on low-temperature protonation of **2**⁻ in the presence of other bidentate ligands.

The flexibility of the M-H-M bridge in the dimeric hydride anions μ-HM₂(CO)₁₀⁻ (M = Cr, Mo, W) and substituted analogues has been demonstrated in the variable configurations that are determined by M,^{2,3} by counterion and crystal packing influences,⁴⁻⁶ and by substituent ligands.^{7,8} The structural possi-

bilities are defined according to the linearity (or lack thereof) of the intersecting vectors OC_{ax}-M...M-CO_{ax} and the staggering or eclipsing of the two equatorial M(CO)₄ units (or M(CO)₃L units) with respect to each other: linear, eclipsed; linear, staggered; bent, eclipsed; and bent, staggered. The last of these predominates by far in the known solid-state structures. The second most common is the linear, eclipsed form, which is observed for the Et₄N⁺ salts of the all-carbonyl hydrides μ-HM₂(CO)₁₀⁻ (M = Cr,⁹ Mo,⁵ and W¹⁰). Thus far there are no known structures in the bent, eclipsed

(1) (a) Texas A&M University. (b) Tulane University. (c) Louisiana State University.

(2) Bau, R.; Teller, R. G.; Kirtley, S. W.; Koetzle, T. F. *Acc. Chem. Res.* **1979**, *12*, 176 and references therein.

(3) Teller, R.; Bau, R. G. *Struct. Bonding (Berlin)* **1982**, *44*, 1.

(4) Petersen, J. L.; Brown, R. K.; and Williams, J. M. *Inorg. Chem.* **1981**, *20*, 158.

(5) Petersen, J. L.; Masino, A.; Stewart, R. P., Jr. *J. Organomet. Chem.* **1981**, *208*, 55.

(6) Roziere, J.; Teulon, P.; Grillone, M. D. *Inorg. Chem.* **1983**, *22*, 557.

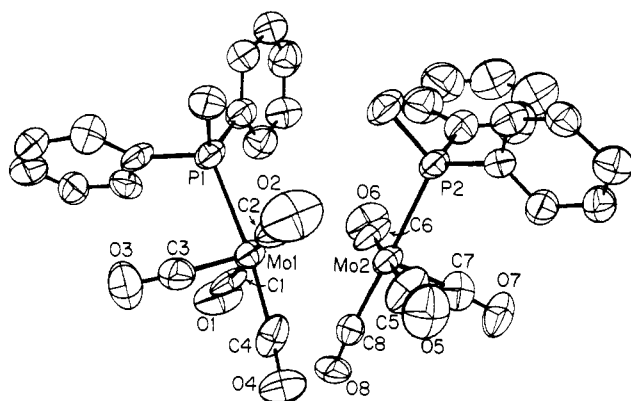
(7) Darensbourg, M. Y.; Atwood, J. L.; Burch, R. R., Jr.; Hunter, W. E.; Walker, N. *J. Am. Chem. Soc.* **1979**, *101*, 2631.

(8) Darensbourg, M. Y.; Atwood, J. L.; Hunter, W. E.; Burch, R. R., Jr. *J. Am. Chem. Soc.* **1980**, *102*, 3290.

(9) Roziere, J.; Williams, J. M.; Stewart, R. P., Jr.; Petersen, J. L.; Dahl, L. F. *J. Am. Chem. Soc.* **1977**, *99*, 4497.

Table I. Elemental Analyses and $\nu(\text{CO})$ Infrared Data for Salts of $(\mu\text{-H})(\mu\text{-Ph}_2\text{P}(\text{CH}_2)_n\text{PPh}_2)\text{Mo}_2(\text{CO})_8^-$

compound	% C		% H		% P		$\nu(\text{CO})^a$, cm^{-1}	
	found	calcd	found	calcd	found	calcd		
1 ⁻ , $\text{Et}_4\text{N}^+\mu\text{-H}[\text{Mo}_2(\text{CO})_8]\text{Ph}_2\text{PCH}_2\text{PPh}_2^-$	50.84	52.86	5.09	4.65	6.25	6.65	2010 m	1990 mw
							1910 s	1837 m
2 ⁻ , $\text{Et}_4\text{N}^+\mu\text{-H}[\text{Mo}_2(\text{CO})_8]\text{Ph}_2\text{P}(\text{CH}_2)_2\text{PPh}_2^-$	53.30	53.35	5.16	4.79	6.01	6.55	2010 m	1990 w
							1913 s	1873 sh
							1830 m	
3 ⁻ , $\text{Et}_4\text{N}^+(\mu\text{-H})[\text{Mo}_2(\text{CO})_8]\text{Ph}_2\text{P}(\text{CH}_2)_3\text{PPh}_2^-$	54.4	53.6	4.9	4.9	5.4	6.5	2011 m	1989 w
							1905 s	1893 sh
							1870 w	1860 w
							1820 m	
4 ⁻ , $\text{Et}_4\text{N}^+\mu\text{-H}[\text{Mo}_2(\text{CO})_8]\text{Ph}_2\text{P}(\text{CH}_2)_4\text{PPh}_2^-$							2010 m	1980 w
							1909 s	1895 w
							1890 w	1866 w
							1828 m	
1 ⁻ , $\text{Ph}_4\text{P}^+\mu\text{-H}[\text{Mo}_2(\text{CO})_8]\text{Ph}_2\text{PCH}_2\text{PPh}_2^-$	59.64	60.01	3.88	3.80	8.31	8.15	2010 m	1990 mw
							1908 s	1837 m
2 ⁻ , $\text{Ph}_4\text{P}^+\mu\text{-H}[\text{Mo}_2(\text{CO})_8]\text{Ph}_2\text{P}(\text{CH}_2)_2\text{PPh}_2^-$	61.41	60.32	4.32	3.93	7.33	8.05	2010 m	1990 w
							1913 s	1873 w
							1830 m	
4 ⁻ , $\text{Ph}_4\text{P}^+\mu\text{-H}[\text{Mo}_2(\text{CO})_8]\text{Ph}_2\text{P}(\text{CH}_2)_4\text{PPh}_2^-$	61.15	60.64	4.33	4.05	7.65	7.95	2010 m	1984 w
							1912 s	1890 w
							1880 vw	1870 vw
							1848 vw	1828 m

^a Measured in THF solution.**Figure 1.** An ORTEP plot of one of the two crystallographically independent anions of $\text{Et}_4\text{N}^+(\mu\text{-H})\text{Mo}_2(\text{CO})_8(\text{PMePh}_2)_2^-$, taken from ref 8.

category and only one report of a linear, staggered structure, $\text{K}^+\mu\text{-HCr}_2(\text{CO})_{10}^-$.⁶

The staggering angle optimum of ca. 45° is seen for several structures including that of $\mu\text{-HMo}_2(\text{CO})_8(\text{PMePh}_2)_2^-$, which has a framework bend of 148° and an average $\text{P}_1\text{-Mo}_1\cdots\text{Mo}_2\text{-P}_2$ torsion angle of 41° .⁸ An ORTEP plot of the X-ray crystal structure of the latter anion (Figure 1) shows an interesting positioning of the two phosphine substituents cis to the hydride bridge and exo to the bent molecular framework. The steric crowding of the two adjacent phosphine ligands is somewhat relieved by the positioning of methyl groups in toward the hydride bridge. Although the refinement of this structure was insufficient to allow for an accurate positioning of the hydrogen bridge, it is expected, by analogy to all other structure determinations in which the hydride was located, to be off the $(\text{OC})_{\text{ax}}\text{M}$ vector intersection point and bound in a closed, three-center, two-electron arrangement.

The relative position of the two phosphine ligands suggested that they might be linked by a hydrocarbon bridge. Thermal reactions of $\text{Et}_4\text{N}^+(\mu\text{-H})\text{Mo}_2(\text{CO})_{10}^-$ with $\text{Ph}_2\text{P}(\text{CH}_2)_n\text{PPh}_2$ have yielded nicely crystalline salts whose spectral characteristics and elemental analyses were readily interpretable according to a $(\mu\text{-H})(\mu\text{-Ph}_2\text{P}(\text{CH}_2)_n\text{PPh}_2)\text{Mo}_2(\text{CO})_8^-$ anion ($n = 1\text{-}4$, referred to as anions 1⁻, 2⁻, 3⁻ and 4⁻, respectively). This report details these preparations, as well as $\nu(\text{CO})$ infrared and NMR spectra, X-ray

crystal structures of two of the salts, and some protonation studies. Our initial goals with these phosphine bridged binuclear hydrides are (1) to determine the effect of the bidentate phosphine bridge length on the structure and flexibility of the Mo-H-Mo grouping and (2) to study the possibility of creating open coordination sites on adjacent metals, held in position by the bidentate bridging phosphines.

Experimental Section

Materials and Methods. All solid reagents and ligands were obtained from standard vendors and used as received. The acid H^+PF_6^- (Aldrich) was in Et_2O solution; CF_3COOH (Sigma) was anhydrous and reagent grade. Solvents used were refluxed over and distilled under N_2 from the following drying agents: tetrahydrofuran (THF), 0.1 M Na/benzophenone blue solution; acetonitrile and methylene chloride, predried over CaCl_2 and distilled from P_2O_5 ; hexane, pretreated with concentrated H_2SO_4 , washed with H_2O , and distilled from CaSO_4 . Reagent grade methanol, chloroform, and toluene were used as received.

Elemental analyses were by Galbraith Laboratories. Infrared spectra were recorded in sealed 0.1-mm NaCl cells either on a Perkin-Elmer 283B spectrophotometer and calibrated against water vapor and CO gas or on an IBM FTIR/85 spectrometer. Reported band positions may have an error of $\pm 2 \text{ cm}^{-1}$. ^1H NMR spectra were obtained on a Varian EM-390, 90-MHz spectrometer.

All preparations and protonation reaction studies were carried out under a dry N_2 atmosphere using standard Schlenk line techniques. Once isolated and dried, the hydride salts were stable in air for moderate periods; however, they were routinely stored in capped vials in a refrigerator.

Preparations and Reactions. **Synthesis of Et_4N^+ and PPh_4^+ Salts of $(\mu\text{-H})(\mu\text{-Ph}_2\text{P}(\text{CH}_2)_n\text{PPh}_2)\text{Mo}_2(\text{CO})_8^-$.** The parent compounds, Et_4N^+ and Ph_4P^+ salts of $(\mu\text{-H})\text{Mo}_2(\text{CO})_{10}^-$, were prepared according to the published method of Hayter.¹¹ Identical synthetic procedures were used for all Et_4N^+ and Ph_4P^+ salts of $(\mu\text{-H})(\mu\text{-Ph}_2\text{P}(\text{CH}_2)_n\text{PPh}_2)\text{Mo}_2(\text{CO})_8^-$, and one example preparation is described. A 100-mL round-bottomed flask fitted with reflux condenser, nitrogen/vacuum inlet, and magnetic stirbar was charged with 1.4 mmol each of $\text{Et}_4\text{N}^+\mu\text{-HMo}_2(\text{CO})_{10}^-$ and $\text{Ph}_2\text{PCH}_2\text{CH}_2\text{PPh}_2$ and 80 mL of THF. This solution was stirred and heated to reflux for 3 h; following that it was cooled to room temperature and filtered through a medium porosity frit. About 100 mL of Et_2O was added, and upon cooling to $+10^\circ\text{C}$ or so for 30 min, a nice yellow powder settled out. If any parent $\mu\text{-HMo}_2(\text{CO})_{10}^-$ was still present the solid was recrystallized from a 1:1 mixture of toluene and methanol. Isolated yields of pure compounds ranged from 50% to 90%. Elemental analyses and $\nu(\text{CO})$ IR data are found in Table I; proton chemical shift values are in Table II.

Protonation Reactions. These reactions were run on a scale to allow for monitoring by solution IR. A typical reaction was as follows. To a

(10) Wilson, R. D.; Graham, S. A.; Bau, R. *J. Organomet. Chem.* **1975**, *91*, C49.(11) Hayter, R. G. *J. Am. Chem. Soc.* **1966**, *88*, 4376.

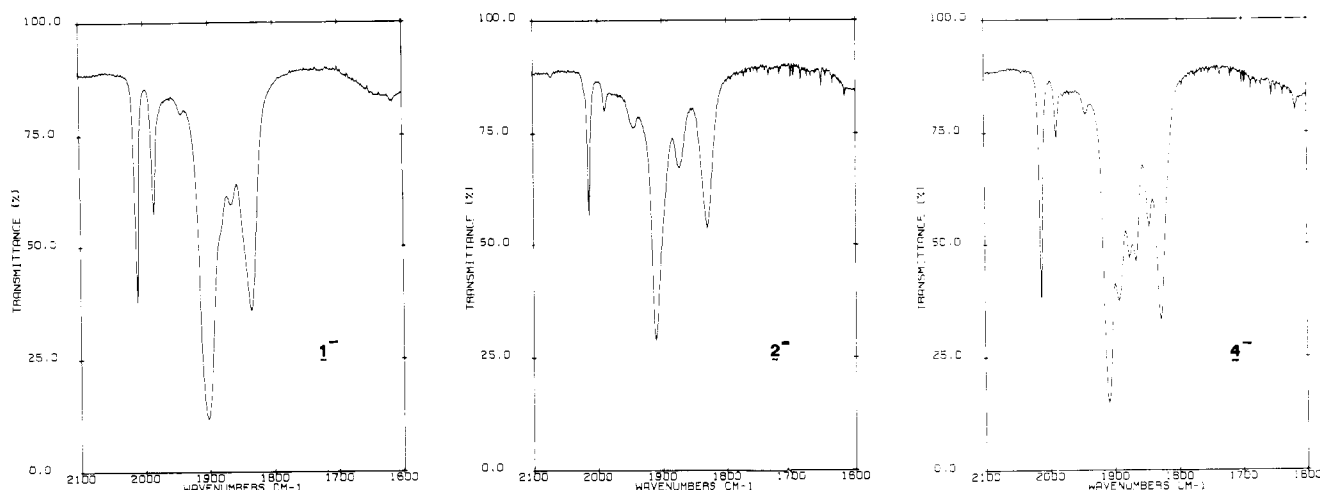


Figure 2. The $\nu(\text{CO})$ infrared spectra of $\text{Ph}_4\text{P}^+\text{1}^-$, $\text{Ph}_4\text{P}^+\text{2}^-$, and $\text{Et}_4\text{N}^+\text{4}^-$ in THF solution.

Table II. ^1H NMR Resonances of Salts of $(\mu\text{-H})(\mu\text{-Ph}_2\text{P}(\text{CH}_2)_n\text{PPh}_2)\text{Mo}_2(\text{CO})_8^-$ in Acetone- d_6 ^a

counterion	<i>n</i>	Mo-H-Mo (<i>J</i> _{P-H})	<i>C</i> ₆ <i>H</i> ₅	(<i>CH</i> ₂) _{<i>n</i>}	counterion
Et_4N^+	1	-11.0 t (18 Hz)	7.56 m 7.23 m	<i>b</i>	1.38 (t of t, C- <i>CH</i> ₃) 3.42 (q, <i>CH</i> ₂ -C)
Et_4N^+	2	-12.0 t (21 Hz)	7.40 m 7.33 m	2.53 d	same
Et_4N^+	4	-10.5 t (18 Hz)	7.67 m 7.33 m	<i>b</i>	same
Ph_4P^+	1	-10.9 t (18 Hz)	7.54 m 7.20 m	3.44 t	7.89 m
Ph_4P^+	2	-11.9 t (21 Hz)	7.23 m	2.57 d	7.82 m
Ph_4P^+	4	-10.4 t (18 Hz)	7.30 m	3.61 m	7.76 m

^a Reported in ppm relative to $\delta(\text{Me}_4\text{Si}) = 0$ ppm. Abbreviations: d = doublet, t = triplet, m = multiplet. ^b These resonance positions are obscured by those of counterion methylene resonances.

50-mL airless flask fitted with serum cap, N_2 /vacuum inlet, and magnetic stirbar was added 10 mL of solvent, 0.1 mmol of dimeric hydride, and 0.3 mmol of any trapping ligand. With rapid stirring, ca. 5–6 mmol of the protonating agent was syringed in and monitoring commenced. Products were identified by their characteristic IR and NMR spectra and, in the case of new compounds, by elemental analysis of the isolated and purified product.

(a) **Protonation of $\text{Et}_4\text{N}^+\text{2}^-$ in the Presence and Absence of CO.** With CO gas bubbling through a THF solution of $\text{Et}_4\text{N}^+\text{2}^-$, H^+PF_6^- in Et_2O solution was discharged immediately into the flask. Complete reaction, with near-quantitative conversion to product according to the spectroscopic monitor, required a period of 14 h. The $\nu(\text{CO})$ IR bands of the product at 2072 w, 1985 w, and 1952 s, br were identical with an authentic sample of $(\mu\text{-Ph}_2\text{P}(\text{CH}_2)_2\text{PPh}_2)\text{Mo}_2(\text{CO})_{10}$ prepared by an alternate route.¹² A similar reaction run in the absence of CO yielded the same product, however, in greatly reduced yields of ca. 30%.

(b) **Protonation of $\text{Ph}_4\text{P}^+\text{2}^-$ in the Presence of *tert*-Butylisocyanide.** This reaction was carried out in CH_2Cl_2 using CF_3COOH as protonating agent and conditions as described above. The reaction was complete within 15 min. The product was isolated (in poor yield) by the addition of CH_3CN to precipitate a white solid. Infrared data and elemental analysis (Table III) are consistent with the formulation $(\mu\text{-Ph}_2\text{P}(\text{CH}_2)_2\text{PPh}_2)[\text{Mo}(\text{CO})_4(\text{CN-}i\text{-Bu})_2]$.

(c) **Protonation of $\text{Ph}_4\text{P}^+\text{2}^-$ in the Presence of Group 5A Bidentate Ligands, $\text{Ph}_2\text{PCH}_2\text{PPh}_2$, $\text{Ph}_2\text{P}(\text{CH}_2)_2\text{PPh}_2$, and $\text{Ph}_2\text{As}(\text{CH}_2)_2\text{AsPh}_2$.** These reactions were carried out as described before, using THF as solvent and H^+PF_6^- in Et_2O as protonating agent. From 30 to 60 min were required for completion as noted by the IR monitor. Solvent was removed in vacuo, and the remaining off-white solids were recrystallized from $\text{CHCl}_3/\text{CH}_3\text{OH}$. Elemental analyses and $\nu(\text{CO})$ IR data are given in Table III and are consistent with the formulation $(\mu\text{-L})(\mu\text{-L}')\text{Mo}_2(\text{CO})_8$. Yields were on the order of 50–60% for the P-donor

derivatives and ca. 20% for the As-donor derivative.

X-ray Crystal Structure Analyses: $[\text{Ph}_4\text{P}^+][(\mu\text{-H})(\mu\text{-Ph}_2\text{P}(\text{CH}_2)_2\text{PPh}_2)\text{Mo}_2(\text{CO})_8^-]$ (**1**) and $[\text{Et}_4\text{N}^+][(\mu\text{-H})(\mu\text{-Ph}_2\text{P}(\text{CH}_2)_4\text{PPh}_2)\text{Mo}_2(\text{CO})_8^-]$ (**4**). The yellow crystals obtained for both salts by crystallization from concentrated solutions in a 1:1 toluene/methanol solvent mixture were mounted in sealed capillary tubes to prevent loss of crystallinity from exposure to the atmosphere. A plot of standard reflection intensities vs. time showed no significant decrease as a result of crystal deterioration for the duration of the data collection process. Data were taken at room temperature on an Enraf-Nonius CAD-4 diffractometer using graphite-monochromated Mo $\text{K}\alpha$ radiation ($\lambda = 0.71073 \text{ \AA}$) and the $\omega/2\theta$ scanning technique with a 3.8° takeoff angle. Twenty-five well-centered reflections, randomly selected from the diffraction lattice, were used to define a monoclinic unit cell for **1** and a triclinic cell for **4**, with lattice constants as given in Table IV. Systematic absences identified the space group as $P2_1/c$ for **1**, while for **4** space group $P\bar{1}$ was determined by successful structure refinement. Data were collected in the range $0^\circ < \theta < 22.5^\circ$ for **1** and $0^\circ < \theta < 25^\circ$ for **4**. In both cases an empirical absorption correction was applied based upon Ψ scans of reflections near $\chi = 90^\circ$. A summary of the data collection, crystal, and final refinement parameters may be found in Table IV.

Since both compounds contain molybdenum, the structures were solved by using the heavy-atom (Patterson) technique.¹³ Both models were refined by using full-matrix weighted least-squares methods. Weights for a given observation were assigned according to the reciprocal of the variance for that observation $(1/\sigma(F_o)^2)$.¹³ For both models, all C_6H_5 phenyl moieties were refined as rigid groups, with initial carbon atomic coordinates made to fit a hexagon.¹⁴ Hydrogen atoms were then placed in calculated positions on the fitted six-carbon ring. Hydrogen atoms of non-phenyl groups were not located from difference Fourier maps but were also placed in calculated positions. All non-hydrogen, non-phenyl atoms were refined anisotropically. In both structures the position of the bridging hydride ion was determined from a difference Fourier map once all other atoms (hydrogen and non-hydrogen) had been located.

As the number of parameters to be refined approached the upper limit tolerated by the SHELX program,¹⁴ it was necessary that those atoms expected to demonstrate similar thermal behavior have their thermal parameters refined as one variable. For compound **4**, all of the carbon atoms in the phenyl rings were refined with one, general isotropic thermal parameter. In addition, the hydrogen atoms of the phenyl groups were combined into one thermal variable. The hydrogen atoms of the terminal methyl groups of the tetraethylammonium cation were also combined as one thermal parameter. For compound **1**, the temperature factors of the carbon atoms of the phenyl groups were refined individually even though the phenyl rings were defined as rigid groups. In structure **1** only the hydrogen atoms of the phenyl groups were joined as one thermal parameter. Fractional coordinates and isotropic thermal parameters for $\text{Ph}_4\text{P}^+\text{1}^-$ and $\text{Et}_4\text{N}^+\text{4}^-$ are given in Tables V and VI, respectively.

The observed and calculated structure factors for **1** and **4** are available as supplementary material, as are atomic positions, thermal parameters, all bond lengths, and bond angles of both structures. The molecular

(13) Stout, G. H.; Jensen, L. H. "X-Ray Structure Determination"; MacMillan: London, 1970.

(14) Sheldrick, G. "SHELX-76, Program for Crystal Structure Determination"; 1976.

(12) Werner, H.; Prinz, R.; Bundschuh, E.; Deckelmann, K. *Angew. Chem., Int. Ed. Engl.* **1966**, *5*, 606.

Table III. Elemental Analyses and $\nu(\text{CO})$ IR Data for $(\mu\text{-LL})_2\text{Mo}_2(\text{CO})_8$ and $(\mu\text{-LL})[\text{Mo}(\text{CO})_4\text{L}']_2$

compound	% C		% H		% P		$\nu(\text{CO}),^a \text{cm}^{-1}$		
	found	calcd	found	calcd	found	calcd			
$(\mu\text{-Ph}_2\text{PCH}_2\text{PPh}_2)(\mu\text{-Ph}_2\text{P}(\text{CH}_2)_2\text{PPh}_2)\text{Mo}_2(\text{CO})_8$	60.90	59.10	4.35	3.84			2020 m	1915 m	1875 s, br
$(\mu\text{-Ph}_2\text{P}(\text{CH}_2)_2\text{PPh}_2)_2\text{Mo}_2(\text{CO})_8$	58.85	59.41	4.05	3.96			2020 m	1933 m	1897 s, br
$(\mu\text{-Ph}_2\text{P}(\text{CH}_2)_2\text{PPh}_2)(\mu\text{-Ph}_2\text{As}(\text{CH}_2)_2\text{AsPh}_2)\text{Mo}_2(\text{CO})_8$	55.40	55.60	3.64	3.70	4.68	4.74	2020 m	1934 m	1900 s, br
$(\mu\text{-Ph}_2\text{P}(\text{CH}_2)_2\text{PPh}_2)[\text{Mo}(\text{CO})_4(\text{C}\equiv\text{NC}(\text{CH}_3)_3)]_2^b$	53.96	53.87	4.71	4.32	6.32	6.32	2017 m	1923 m	1890 s, br

^a Measured in THF solution. ^b The C≡N stretch of the ligand is at 2136 cm^{-1} .

Table IV. Crystal Data for $[\text{Ph}_4\text{P}^+][(\mu\text{-H})(\mu\text{-Ph}_2\text{P}(\text{CH}_2)_2\text{PPh}_2)\text{Mo}_2(\text{CO})_8]^-$ (1) and $[\text{Et}_4\text{N}^+][(\mu\text{-H})(\mu\text{-Ph}_2\text{P}(\text{CH}_2)_4\text{PPh}_2)\text{Mo}_2(\text{CO})_8]^-$ (4)

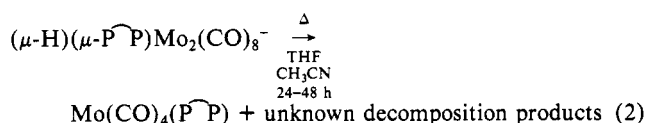
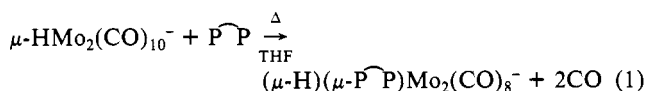
empirical formula	$\text{Mo}_2\text{P}_3\text{C}_{57}\text{O}_8\text{H}_{43}$ (1)	$\text{Mo}_2\text{P}_2\text{N}_1\text{C}_{44}\text{O}_8\text{H}_{49}$ (4)
formula weight	1139.7	972.6
crystal dimensions, mm	$0.28 \times 0.36 \times 0.56$	$0.20 \times 0.32 \times 0.48$
crystal system	monoclinic	triclinic
space group	$P2_1/c$	$P\bar{1}$
cell dimensions		
<i>a</i> , Å	13.886 (6)	8.760 (2)
<i>b</i> , Å	18.545 (9)	13.940 (4)
<i>c</i> , Å	20.156 (6)	19.686 (4)
α , deg	90	105.75 (2)
β , deg	91.03 (4)	93.59 (2)
γ , deg	90	97.38 (2)
volume, Å ³	5190 (4)	2282 (1)
<i>Z</i>	4	2
density (calcd)	1.46	1.42
abs. coeff, μ , cm^{-1}	5.90	5.52
reflections collected	7390	8230
unique reflections	5723	6752
reflections used in analysis ^a	4402	4720
parameters refined	301	358
final agreement factors ^b		
<i>R</i>	0.0413	0.0471
<i>R</i> _w	0.0448	0.0538

^a $|I_o| > 3\sigma(I_o)$. ^b $R(F) = \sum |F_o - |F_c|| / \sum F_o$; $R(wF) = \{\sum w(F_o - |F_c|)^2 / \sum wF_o^2\}^{1/2}$

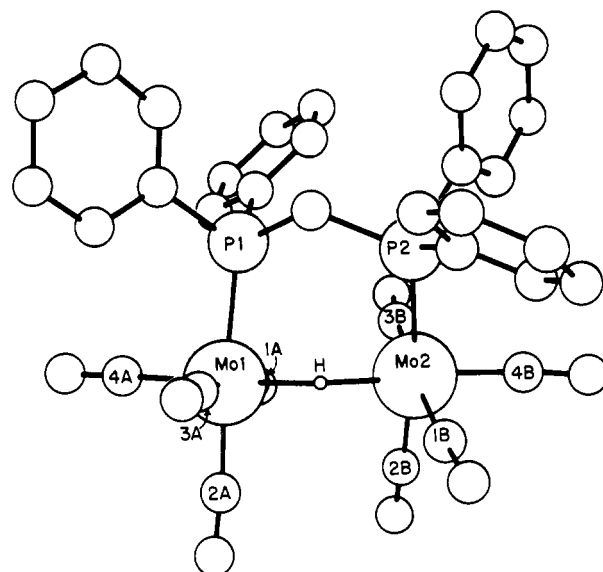
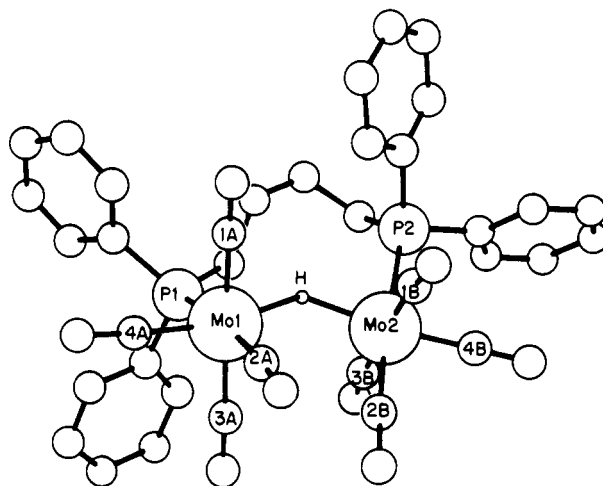
diagrams, Figures 3 and 4, were generated by using the PLUTO program of the Cambridge Crystal System of Programs.¹⁵

Results and Discussion

Synthesis and Spectral Properties. Of the three 6B $\mu\text{-HM}_2(\text{CO})_{10}^-$, the molybdenum derivative is least stable, both toward dimer dissociation and toward CO lability. Advantage was taken of the latter to synthesize the phosphine-substituted dimers by direct thermal substitution (eq 1). Once isolated, the title compounds are stable in air and decompose only slowly (1–2 days) in refluxing THF or CH_3CN , to yield as CO-containing product, $\text{Mo}(\text{CO})_4(\text{P}\text{P})$ (eq 2). Their reactions with acids are reviewed below.



There are four prominent $\nu(\text{CO})$ IR absorptions for the $(\mu\text{-H})(\mu\text{-Ph}_2\text{P}(\text{CH}_2)_n\text{PPh}_2)\text{Mo}_2(\text{CO})_8^-$ salts: two medium to weak narrow bands around 2000 cm^{-1} , a strong band around 1910 cm^{-1} , and a medium band at ca. 1820 cm^{-1} . The simplest spectrum is observed for $n = 1$, or 1⁻, and the region between the lower two bands shows increasing complexity as the *n* value or chain length

**Figure 3.** The molecular structure diagram of $\text{Ph}_4\text{P}^+(\mu\text{-H})(\mu\text{-Ph}_2\text{PCH}_2\text{PPh}_2)\text{Mo}_2(\text{CO})_8^-$ (1⁻).**Figure 4.** The molecular structure diagram of $\text{Et}_4\text{N}^+(\mu\text{-H})(\mu\text{-Ph}_2\text{P}(\text{CH}_2)_4\text{PPh}_2)\text{Mo}_2(\text{CO})_8^-$ (4⁻).

increases (see Figure 2). The solution spectrum of nonbridged $(\mu\text{-H})[\text{Mo}(\text{CO})_4\text{PMePh}_2]_2^-$ (Figure 1) is nearly identical with that of 2⁻ or the $\text{Ph}_2\text{P}(\text{CH}_2)_2\text{PPh}_2$ derivative.⁸

The monomeric hydride *cis*- $\text{HW}(\text{CO})_4\text{PMe}_3^-$ has been synthesized and its $\nu(\text{CO})$ pattern (1969 cm^{-1} , m, sharp; 1842 cm^{-1} , s, br; 1805 m) was interpreted according to a pseudo C_{2v} symmetry (A' , $A' + A''$, A'' , respectively).¹⁶ The local symmetry of molecular anions 1⁻–4⁻ is also pseudo C_{2v} . Although a local symmetry approximation was used with success to assign the spectra of $(\mu\text{-H})\text{M}_2(\text{CO})_{10}^-$ anions,¹⁷ it appears to be inappropriate here. It is noteworthy that the Nujol mull spectrum of Et_4N^+2^- has an

(16) Slater, S. G.; Lusk, R.; Schumann, B. F.; Darensbourg, M. Y. *Organometallics* **1982**, *1*, 1662.

(17) Darensbourg, D. J.; Burch, R. R., Jr.; Darensbourg, M. Y. *Inorg. Chem.* **1978**, *17*, 2677.

(15) Kennard, O. Cambridge Crystallographic Database, University Chemical Laboratory, Cambridge, England, 1981.

Table V. Atomic Positional Parameters ($\times 10^4$) and Isotropic Thermal Parameters ($\times 10^3$)^a for $\text{Ph}_4\text{P}^+(\mu\text{-H})(\mu\text{-Ph}_2\text{PCH}_2\text{PPh}_2)\text{Mo}_2(\text{CO})_8^-$

atom	x	y	z	u	atom	x	y	z	u
Mo(1)	2065 (1)	3703 (1)	1587 (1)	39 (1)	C(70)	8413 (3)	3291 (3)	4595 (2)	66 (2)
C(1A)	8033 (5)	5245 (4)	8357 (3)	47 (2)	C(71)	9104 (3)	3502 (3)	4140 (2)	86 (3)
O(1A)	8055 (4)	4621 (3)	8345 (3)	83 (3)	C(72)	10058 (3)	3281 (3)	4225 (2)	77 (2)
C(2A)	9234 (6)	6461 (4)	8017 (4)	60 (3)	C(73)	10323 (3)	2848 (3)	4764 (2)	78 (2)
O(2A)	9988 (4)	6556 (3)	7798 (4)	104 (3)	C(74)	9632 (3)	2637 (3)	5219 (2)	65 (2)
C(3A)	8568 (6)	6271 (4)	9293 (4)	67 (3)	C(75)	8678 (3)	2858 (3)	5135 (2)	47 (2)
O(3A)	8975 (6)	6236 (4)	9795 (3)	122 (3)	C(80)	8922 (3)	3198 (3)	6665 (2)	67 (2)
C(4A)	6671 (6)	6143 (4)	8883 (4)	55 (3)	C(81)	9196 (3)	3352 (3)	7319 (2)	78 (2)
O(4A)	6004 (4)	6010 (3)	9185 (3)	90 (3)	C(82)	8734 (3)	3011 (3)	7842 (2)	75 (2)
P(1)	7201 (1)	6433 (1)	7273 (1)	35 (1)	C(83)	7999 (3)	2516 (3)	7711 (2)	95 (3)
C(10)	8497 (3)	5436 (2)	6724 (2)	56 (2)	C(84)	7725 (3)	2362 (3)	7057 (2)	79 (2)
C(11)	8914 (3)	5055 (2)	6206 (2)	61 (2)	C(85)	8187 (3)	2703 (3)	6534 (2)	45 (2)
C(12)	8511 (3)	5092 (2)	5567 (2)	67 (2)	C(99)	7455 (4)	7314 (3)	6884 (3)	37 (2)
C(13)	7691 (3)	5511 (2)	5447 (2)	67 (2)	H(10)	8809 (3)	5407 (2)	7218 (2)	120 (5)
C(14)	7275 (3)	5892 (2)	5965 (2)	51 (2)	H(11)	9548 (3)	4731 (2)	6299 (2)	120 (5)
C(15)	7678 (3)	5855 (2)	6603 (2)	39 (2)	H(12)	8833 (3)	4797 (2)	5166 (2)	120 (5)
C(20)	5291 (3)	6752 (2)	6829 (2)	48 (2)	H(13)	7380 (3)	5540 (2)	4953 (2)	120 (5)
C(21)	4303 (3)	6618 (2)	6804 (2)	57 (2)	H(14)	6641 (3)	6216 (2)	5872 (2)	120 (5)
C(22)	3927 (3)	6017 (2)	7126 (2)	63 (2)	H(20)	5581 (3)	7217 (2)	6580 (2)	120 (5)
C(23)	4541 (3)	5550 (2)	7474 (2)	70 (2)	H(21)	3828 (3)	6979 (2)	6534 (2)	120 (5)
C(24)	5530 (3)	5684 (2)	7499 (2)	57 (2)	H(22)	3162 (3)	5914 (2)	7106 (2)	120 (5)
C(25)	5905 (3)	6285 (2)	7177 (2)	37 (1)	H(23)	4251 (3)	5085 (2)	7723 (2)	120 (5)
Mo(2)	2864 (1)	1978 (1)	1428 (1)	37 (1)	H(24)	6005 (3)	5323 (2)	7769 (2)	120 (5)
C(2A)	6588 (5)	8985 (4)	8708 (3)	48 (3)	H(30)	7519 (3)	9600 (2)	7692 (2)	120 (5)
O(2A)	6352 (4)	9574 (3)	8796 (3)	77 (2)	H(31)	8666 (3)	10536 (2)	7331 (2)	120 (5)
C(2B)	7123 (5)	7769 (4)	9533 (4)	49 (3)	H(32)	9821 (3)	10267 (2)	6443 (2)	120 (5)
O(2B)	7088 (4)	7609 (3)	10079 (3)	71 (2)	H(33)	9827 (3)	9061 (2)	5916 (2)	120 (5)
C(3B)	5803 (5)	7571 (4)	8507 (3)	48 (2)	H(34)	8680 (3)	8125 (2)	6277 (2)	120 (5)
O(3B)	5027 (4)	7355 (3)	8502 (3)	67 (2)	H(40)	5207 (3)	8550 (2)	7765 (1)	120 (5)
C(4B)	8396 (5)	8552 (4)	8714 (3)	50 (3)	H(41)	3725 (3)	8930 (2)	7161 (1)	120 (5)
O(4B)	9048 (4)	8905 (3)	8832 (3)	90 (3)	H(42)	3732 (3)	9065 (2)	5940 (1)	120 (5)
P(2)	7147 (1)	8149 (1)	7333 (1)	35 (1)	H(43)	5221 (3)	8820 (2)	5322 (1)	120 (5)
C(30)	8023 (3)	9483 (2)	7304 (2)	56 (2)	H(44)	6704 (3)	8441 (2)	5926 (1)	120 (5)
C(31)	8669 (3)	10010 (2)	7101 (2)	74 (2)	H(50)	8826 (3)	1447 (3)	4997 (2)	120 (5)
C(32)	9320 (3)	9858 (2)	6600 (2)	65 (2)	H(51)	8521 (3)	144 (3)	4832 (2)	120 (5)
C(33)	9324 (3)	9179 (2)	6303 (2)	60 (2)	H(52)	7060 (3)	-418 (3)	5291 (2)	120 (5)
C(34)	8677 (3)	8651 (2)	6507 (2)	50 (2)	H(53)	5903 (3)	324 (3)	5914 (2)	120 (5)
C(35)	8026 (3)	8803 (2)	7008 (2)	36 (1)	H(54)	6207 (3)	1628 (3)	6079 (2)	120 (5)
C(40)	5210 (3)	8609 (2)	7232 (1)	46 (2)	H(60)	7102 (3)	3890 (3)	6247 (2)	120 (5)
C(41)	4375 (3)	8823 (2)	6892 (1)	60 (2)	H(61)	5703 (3)	4659 (3)	5951 (2)	120 (5)
C(42)	4379 (3)	8899 (2)	6203 (1)	64 (2)	H(62)	4528 (3)	4258 (3)	5090 (2)	120 (5)
C(43)	5218 (3)	8761 (2)	5855 (1)	59 (2)	H(63)	4753 (3)	3087 (3)	4524 (2)	120 (5)
C(44)	6054 (3)	8547 (2)	6195 (1)	45 (2)	H(64)	6152 (3)	2317 (3)	4820 (2)	120 (5)
C(45)	6050 (3)	8471 (2)	6884 (1)	39 (2)	H(70)	7674 (3)	3462 (3)	4530 (2)	120 (5)
P(3)	7783 (1)	2553 (1)	5697 (1)	45 (1)	H(71)	8899 (3)	3837 (3)	3723 (2)	120 (5)
C(50)	8188 (3)	1202 (3)	5197 (2)	63 (2)	H(72)	10593 (3)	3445 (3)	3872 (2)	120 (5)
C(51)	8016 (3)	467 (3)	5104 (2)	75 (2)	H(73)	11062 (3)	2677 (3)	4829 (2)	120 (5)
C(52)	7193 (3)	151 (3)	5363 (2)	69 (2)	H(74)	9837 (3)	2302 (3)	5637 (2)	120 (5)
C(53)	6540 (3)	569 (3)	5714 (2)	71 (2)	H(80)	9280 (3)	3462 (3)	6260 (2)	120 (5)
C(54)	6712 (3)	1304 (3)	5807 (2)	64 (2)	H(81)	9765 (3)	3735 (3)	7420 (2)	120 (5)
C(55)	7536 (3)	1620 (3)	5546 (2)	49 (2)	H(82)	8946 (3)	3130 (3)	8348 (2)	120 (5)
C(60)	6590 (3)	3714 (3)	5871 (2)	64 (2)	H(83)	7641 (3)	2252 (3)	8115 (2)	120 (5)
C(61)	5801 (3)	4148 (3)	5705 (2)	77 (2)	H(84)	7156 (3)	1979 (3)	6955 (2)	120 (5)
C(62)	5139 (3)	3922 (3)	5219 (2)	79 (2)	H(99A)	7056 (4)	7327 (3)	6416 (3)	120 (5)
C(63)	5265 (3)	3262 (3)	4900 (2)	82 (3)	H(99B)	8219 (4)	7332 (3)	6795 (3)	120 (5)
C(64)	6054 (3)	2828 (3)	5067 (2)	64 (2)	H(100)	8010 (38)	7313 (31)	8346 (27)	52 (17)
C(65)	6716 (3)	3055 (3)	5552 (2)	50 (2)					

^a Anisotropic thermal parameters are in the supplementary material as Table S5.

identical pattern and band positions as the THF solution spectrum. The assignment, which should be facilitated by the good solid-state structural information presented below, as well as the fact that the solid-state structures appear to be rigorously maintained in solution, remains to be done.

The proton chemical shifts of the monomeric and dimeric hydrides $\text{HMo}(\text{CO})_5^-$ and $(\mu\text{-H})\text{Mo}_2(\text{CO})_{10}^-$ are 4.0 and 12.2 ppm upfield from Me_4Si , respectively.¹⁸ The phosphorus ligand substituted monomeric molybdenum hydride is currently unknown; however, the known *cis*- $\text{HW}(\text{CO})_4\text{P}(\text{OMe})_3^-$ has its hydride resonance at -4.5 ppm (doublet, $J_{\text{P-H}} = 36 \text{ Hz}$).¹⁶ The dimeric analogue $(\mu\text{-H})[\text{W}(\text{CO})_4\text{P}(\text{OMe})_3]_2^-$ has a triplet centered at

-11.8 ppm with $J_{\text{P-H}} = 21 \text{ Hz}$,¹⁶ and the parent anion $(\mu\text{-H})\text{W}_2(\text{CO})_{10}^-$ has a chemical shift of -12.6 ppm.¹¹ Thus, as expected, the hydride resonances of the title anions are also triplets with $J_{\text{P-H}} = 18\text{--}21 \text{ Hz}$, which are centered from 10 to 12 ppm upfield from Me_4Si . To summarize, (1) the chemical shift of a bridging hydride ligand is to considerably higher field strengths than that of a terminal hydride; (2) in this series of hydrido anions the presence of the phosphine ligand has little influence on the chemical shift value in either terminal or bridging hydrides; and (3) the P-H coupling constant in dimeric hydrides is roughly half the value of monomeric hydrides.

The X-ray Structures of $\text{Et}_4\text{N}^+(\mu\text{-H})(\mu\text{-Ph}_2\text{PCH}_2\text{PPh}_2)\text{Mo}_2(\text{CO})_8^-$ (1) and $\text{PPh}_4^+(\mu\text{-H})(\mu\text{-Ph}_2\text{P}(\text{CH}_2)_4\text{PPh}_2)\text{Mo}_2(\text{CO})_8^-$ (4). Lists of the pertinent interatomic distances and angles in anions 1⁻ and 4⁻ are given in Table VII and referenced to the numbering

(18) Darensbourg, M. Y.; Slater, S. G. *J. Am. Chem. Soc.* **1981**, *103*, 5914.

Table VI. Atomic Positional Parameters ($\times 10^4$) and Isotropic Thermal Parameters ($\times 10^3$)^a for $\text{Et}_4\text{N}^+(\mu\text{-H})(\mu\text{-Ph}_2\text{P}(\text{CH}_2)_4\text{PPh}_2)\text{Mo}_2(\text{CO})_8^-$

atom	x	y	z	u	atom	x	y	z	u
Mo(1)	3012 (1)	1364 (1)	3060 (1)	44 (1)	C(37)	10336 (12)	2741 (9)	5644 (6)	114 (6)
P(1)	4843 (2)	131 (1)	2611 (1)	47 (1)	C(38)	12037 (14)	3290 (12)	5658 (7)	134 (7)
C(1A)	1339 (9)	943 (5)	2231 (4)	59 (3)	C(39)	10051 (14)	3734 (9)	6882 (5)	108 (5)
O(1A)	319 (7)	737 (5)	1803 (3)	94 (3)	C(40)	10411 (16)	2837 (10)	7173 (6)	134 (6)
C(2A)	1706 (9)	2345 (7)	3540 (4)	67 (3)	H(5A)	6969 (8)	-121 (5)	1891 (4)	52 (18)
O(2A)	994 (7)	2902 (5)	3871 (3)	103 (3)	H(5B)	6837 (8)	1171 (5)	2228 (4)	49 (17)
C(3A)	4481 (9)	1900 (6)	3959 (4)	58 (3)	H(6A)	4330 (8)	836 (5)	1420 (4)	80 (24)
O(3A)	5197 (7)	2213 (5)	4495 (3)	89 (3)	H(6B)	4789 (8)	-373 (5)	1023 (4)	49 (17)
C(4A)	2021 (8)	296 (6)	3420 (4)	64 (3)	H(7A)	7696 (9)	2000 (5)	1557 (4)	68 (21)
O(4A)	1474 (7)	-382 (5)	3607 (4)	98 (3)	H(7B)	7577 (9)	2131 (5)	689 (4)	128 (35)
MO(2)	4872 (1)	3456 (1)	2620 (1)	43 (1)	H(8A)	5518 (10)	739 (5)	316 (4)	78 (23)
P(2)	5557 (2)	2860 (1)	1346 (1)	44 (1)	H(8B)	7180 (10)	398 (5)	686 (4)	57 (20)
C(1B)	2737 (11)	3724 (7)	2337 (4)	74 (3)	H(9)	2020 (6)	-796 (3)	1700 (3)	169 (9)
O(1B)	1578 (9)	3952 (6)	2225 (4)	133 (4)	H(10)	1033 (6)	-2536 (3)	964 (3)	169 (9)
C(2B)	4532 (10)	4032 (5)	3615 (4)	67 (3)	H(11)	2514 (6)	-3922 (3)	999 (3)	169 (9)
O(2B)	4391 (9)	4431 (5)	4208 (3)	107 (3)	H(12)	4982 (6)	-3568 (3)	1770 (3)	169 (9)
C(3B)	6984 (11)	3272 (7)	2956 (4)	79 (4)	H(13)	5969 (6)	-1828 (3)	2505 (3)	169 (9)
O(3B)	8210 (9)	3223 (7)	3160 (5)	152 (5)	H(15)	4316 (4)	-889 (4)	3691 (3)	169 (9)
C(4B)	5672 (9)	4813 (6)	2608 (4)	60 (3)	H(16)	5889 (4)	-900 (4)	4777 (3)	169 (9)
O(4B)	6132 (7)	5650 (4)	2629 (3)	83 (2)	H(17)	8576 (4)	3 (4)	5049 (3)	169 (9)
C(5)	6185 (8)	428 (5)	1996 (4)	54 (3)	H(18)	9690 (4)	916 (4)	4235 (3)	169 (9)
C(6)	5262 (8)	401 (5)	1295 (4)	57 (3)	H(19)	8117 (4)	927 (4)	3149 (3)	169 (9)
C(7)	6923 (9)	1927 (5)	1090 (4)	61 (3)	H(21)	2363 (6)	2038 (4)	1347 (2)	169 (9)
C(8)	6240 (10)	829 (5)	801 (4)	62 (3)	H(22)	202 (6)	1291 (4)	403 (2)	169 (9)
C(9)	2667 (6)	-1400 (3)	1715 (3)	69 (9)	H(23)	589 (6)	1202 (4)	-846 (2)	169 (9)
C(10)	2110 (6)	-2381 (3)	1301 (3)	69 (9)	H(24)	3138 (6)	1860 (4)	-1151 (2)	169 (9)
C(11)	2945 (6)	-3162 (3)	1320 (3)	69 (9)	H(25)	5299 (6)	2607 (4)	-207 (2)	169 (9)
C(12)	4336 (6)	-2963 (3)	1754 (3)	69 (9)	H(27)	4567 (4)	4455 (4)	800 (3)	169 (9)
C(13)	4892 (6)	-1982 (3)	2169 (3)	69 (9)	H(28)	6000 (4)	5893 (4)	480 (3)	169 (9)
C(14)	4058 (6)	-1201 (3)	2149 (3)	69 (9)	H(29)	8864 (4)	6166 (4)	605 (3)	169 (9)
C(15)	5488 (4)	-495 (4)	3810 (3)	69 (9)	H(30)	10295 (4)	5001 (4)	1048 (3)	169 (9)
C(16)	6375 (4)	-501 (4)	4422 (3)	69 (9)	H(31)	8861 (4)	3564 (4)	1368 (3)	169 (9)
C(17)	7889 (4)	7 (4)	4575 (3)	69 (9)	H(33A)	7970 (12)	2098 (8)	6260 (6)	108 (31)
C(18)	8517 (4)	522 (4)	4117 (3)	69 (9)	H(33B)	7375 (12)	2438 (8)	5497 (6)	122 (36)
C(19)	7631 (4)	528 (4)	3504 (3)	69 (9)	H(34A)	5543 (16)	2726 (10)	6293 (7)	146 (5)
C(20)	6116 (4)	19 (4)	3351 (3)	69 (9)	H(34B)	6505 (16)	3887 (10)	6231 (7)	146 (5)
C(21)	2532 (6)	1999 (4)	802 (2)	69 (9)	H(34A)	6681 (162)	3471 (102)	6861 (63)	146 (5)
C(22)	1314 (6)	1578 (4)	270 (2)	69 (9)	H(35A)	8506 (12)	4749 (7)	6286 (5)	124 (37)
C(23)	1532 (6)	1528 (4)	-434 (2)	69 (9)	H(35B)	10325 (12)	4761 (7)	5949 (5)	88 (27)
C(24)	2969 (6)	1899 (4)	-606 (2)	69 (9)	H(36A)	8170 (12)	4833 (9)	5089 (6)	146 (5)
C(25)	4187 (6)	2320 (4)	-74 (2)	69 (9)	H(36B)	7296 (12)	3638 (9)	5125 (6)	146 (5)
C(26)	3969 (6)	2370 (4)	630 (2)	69 (9)	H(36A)	8978 (128)	3716 (81)	4625 (62)	146 (5)
C(27)	5816 (4)	4574 (4)	854 (3)	69 (9)	H(37A)	10399 (12)	2070 (9)	5811 (6)	102 (33)
C(28)	6624 (4)	5385 (4)	674 (3)	69 (9)	H(37B)	9786 (12)	2534 (9)	5107 (6)	81 (25)
C(29)	8239 (4)	5539 (4)	744 (3)	69 (9)	H(38A)	12728 (14)	3353 (12)	6146 (7)	146 (5)
C(30)	9045 (4)	4882 (4)	994 (3)	69 (9)	H(38B)	12039 (4)	4031 (12)	5584 (7)	146 (5)
C(31)	8237 (4)	4072 (4)	1174 (3)	69 (9)	H(38C)	12390 (137)	2838 (89)	5260 (64)	146 (5)
C(32)	6623 (4)	3918 (4)	1104 (3)	69 (9)	H(39A)	11108 (14)	4253 (9)	6933 (5)	113 (34)
N(1)	9395 (7)	3371 (4)	6108 (3)	64 (2)	H(39B)	9219 (4)	4117 (9)	7192 (5)	256 (85)
C(33)	7806 (12)	2722 (8)	6051 (6)	99 (5)	H(40A)	11092 (16)	2393 (10)	6806 (6)	146 (5)
C(34)	6608 (16)	3252 (10)	6437 (7)	122 (6)	H(40B)	9321 (16)	2385 (10)	7185 (6)	146 (5)
C(35)	9198 (12)	4323 (7)	5914 (5)	98 (5)	H(40C)	10907 (138)	2995 (89)	7591 (64)	146 (5)
C(36)	8385 (12)	4111 (9)	5145 (6)	108 (5)	H(50)	4136 (72)	2083 (48)	2495 (36)	65 (20)

^a Anisotropic thermal parameters are in the supplementary material as Table S6.

schemes of the molecular diagrams of Figures 3 and 4. A complete listing of all bond lengths and bond angles is deposited as supplementary material. In both structures the six-coordinate Mo atoms reside in roughly octahedral environments. The Mo-C-O linkages deviate from linearity by no more than 0-4° as is usual for metal carbonyl structures. The Mo-C bonds may be divided into two groups of similar lengths. Those Mo-C bonds of carbonyl groups trans to each other are in the 2.01-2.03 Å range and those trans to either the P-donor site or the bridging hydride are slightly shorter at 1.95-1.98 Å. The C-O distances range from 1.13 to 1.17 Å and show no trends. There are no obvious interionic contacts that might influence the structure. The deviations from strict octahedral coordination symmetry about each Mo seem to be readily rationalized by the binding requirements of the bridging phosphine ligands (vide infra).

On initial inspection, the two new structures are very similar to the bridging hydride anion substituted by two monodentate phosphine ligands, $(\mu\text{-H})\text{Mo}_2(\text{CO})_8(\text{PMePh}_2)_2$, which inspired this study. Several pertinent structural features are compared

in Table VIII along with those of $(\mu\text{-H})\text{Mo}_2(\text{CO})_9\text{PPh}_3^-$ and the all carbonyl parent, $(\mu\text{-H})\text{Mo}_2(\text{CO})_{10}^-$. Structures of the latter are available as both the K crypt-222⁺ salt and the PPN⁺ salt.⁵ The Et_4N^+ salt was shown to be isomorphous with the Cr and W analogues, which are of the linear, eclipsed conformation.² Thus all the known completed structures of dimolybdenum bridging hydrides are of the bent, staggered configuration and are contained in Table VIII. The Mo-H-Mo angles of ca. 130° are more acute than the framework bend angles of ca. 150-160°, confirming the accepted closed, 3-center bonding arrangement of the hydride bridge.² The staggering appears to be of two types, either 22-24° as in the PPN⁺ salt of $(\mu\text{-H})\text{Mo}_2(\text{CO})_{10}^-$ and I⁻ or ca. 45° as in the other three structures. We have defined the degree of staggering in the new structures I⁻ and 4⁻ as the P₁-Mo₁-Mo₂-P₂ torsion angle of the P₁-Mo₁...Mo₂-P₂ unit. As Figure 5 shows, the slight distortions from strict octahedral symmetry would lead to different twist angles should other defining units be chosen. Nevertheless, there is a significant difference between ca. 45°, the optimum twist, and ca. 22°, an intermediate

Table VII. Interatomic Distances in the Anions of $\text{Ph}_2\text{P}^-(\mu\text{-H})(\mu\text{-Ph}_2\text{PCH}_2\text{PPh}_2)\text{Mo}_2(\text{CO})_{10}^-$ (**1**) and $\text{Et}_3\text{N}^+(\mu\text{-H})(\mu\text{-Ph}_2\text{P}(\text{CH}_2)_4\text{PPh}_2)\text{Mo}_2(\text{CO})_{10}^-$ (**4**)

atoms		distances, Å	
		1 ⁻	4 ⁻
Mo(1)	Mo(2)	3.4028 (8)	3.4995 (8)
Mo(1)	H	1.89 (6)	1.92 (7)
Mo(2)	H	1.85 (6)	1.88 (7)
Mo(1)	P	2.513 (2)	2.522 (2)
Mo(1)	C1A	2.029 (8)	2.029 (8)
Mo(1)	C2A	1.964 (8)	1.977 (9)
Mo(1)	C3A	2.010 (8)	2.023 (7)
Mo(1)	C4A	1.959 (7)	1.946 (9)
Mo(2)	P	2.509 (2)	2.556 (2)
Mo(2)	C1B	2.023 (7)	2.03 (1)
Mo(2)	C2B	1.994 (7)	1.962 (8)
Mo(2)	C3B	2.034 (7)	2.00 (1)
Mo(2)	C4B	1.962 (8)	1.938 (8)

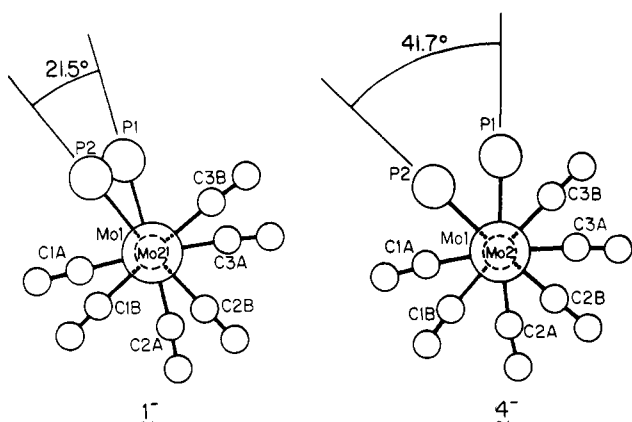


Figure 5. The "end-on" view of **1**⁻ and **4**⁻ showing the degree of staggering in each molecular anion, i.e., the dihedral angles noted.

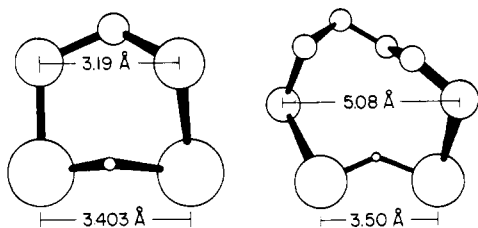


Figure 6. The two bridges of **1**⁻ and **4**⁻. The apex of the hydride bridge in **1**⁻ is directed ca. 90° from that of the P-CH₂-P bridge, whereas in **4**⁻ the apices of both bridges are roughly in the same direction.

twist angle. The largest Mo...Mo distance is observed for **4**⁻, consistent with the large bite of the butylenediphos ligand. Next largest is that of the monosubstituted PPh₃ derivative, followed by the disubstituted PMePh₂ derivative. Anion **1**⁻, containing the diphenylphosphinomethane (DPM) bridge, has the smallest Mo...Mo distance of all the known structures, including the nonsubstituted all carbonyl parent anions. Nevertheless, at 3.40 Å this distance is considerably greater than that of the Mo-Mo single bond distance of 3.12 Å measured for Mo₂(CO)₁₀²⁻.¹⁹

Noted in Figure 6 are the distances between the coordinated phosphorus atoms in both **1**⁻ and **4**⁻. Whereas both ligands accomplish their mission of bridging the binuclear hydrides, the larger bridging ligand appears to be underextended by 1.6 Å and the small bridge results in a P...P distance about 0.2 Å less than the Mo...Mo distance. As further evidence of the heroic and successful attempt of the DPM ligand to span the Mo...Mo separation, the P-C-P angle opens to 119.1 (3)° in **1**⁻. Such a display of the commodious nature of the DPM ligand is reminiscent of its

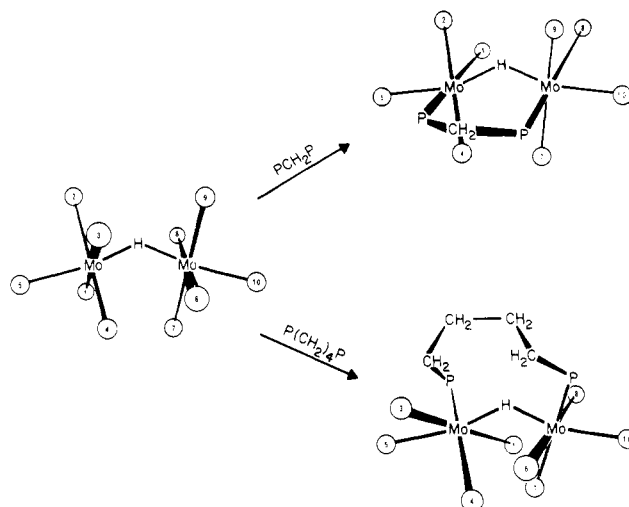


Figure 7. Stick drawings of the coordination site positions in $(\mu\text{-H})\text{Mo}_2(\text{CO})_{10}^-$ (taken from the ORTEP plot of the $\text{PPN}^+(\mu\text{-H})\text{Mo}_2(\text{CO})_{10}^-$)⁵ of **1**⁻ and of **4**⁻. The calculated site separation distances in Table IX are referenced to these drawings.

usefulness in the development of A-frame rhodium dimer chemistry.²⁰ Large nonbonded Rh...Rh separations such as 3.24 Å in Rh₂Cl₂(CO)₂(DPM)₂ for example lead to a P-C-P angle of 117° and a P...P inter donor site distance of 3.13 Å.²¹ The short Rh-Rh bonding distances of ca. 2.7-2.8 Å are still accommodated by the DPM ligand where P-C-P angles of 110-112° are typical and P-P distances at ca. 3.0 Å are slightly greater than the Rh-Rh distances.²²

Comparison of the molecular diagram of **4**⁻, Figure 3, and of the analogous ORTEP plot of $(\mu\text{-H})\text{Mo}_2(\text{CO})_8(\text{PMePh}_2)_2$, Figure 1, suggests that the methyl substituents of the two phosphine ligands of the latter have indeed been substituted by the butylene bridge which goes over the top of the hydride bridge in a bilevel bridge arrangement. Although the data in Table VII suggest substantial similarity in all the structures, there is a subtle but important difference between **1**⁻ and **4**⁻ with respect to the bridge positions relative to one another. As magnified by Figure 6, the methylene phosphine bridge of **1**⁻ is almost perpendicular to the hydride bridge. Parallel, rather than bilevel, double bridges are observed. These differences can be rationalized on the basis of distances between coordination site positions on adjacent Mo atoms in the bent, staggered form of the parent $(\mu\text{-H})\text{Mo}_2(\text{CO})_{10}^-$.

The stick drawing of $\mu\text{-HMo}_2(\text{CO})_{10}^-$ in Figure 7 is a representation of the anion in its most bent, staggered form, as its PPN^+ salt.⁵ We have calculated the distances between appropriate pairs of points of ca. 2.5 Å from the Mo atoms along the Mo-CO vectors for this anion as well as for the derivatives **1**⁻ and **4**⁻, Table IX.²³ The parent anion shows site separations in roughly three categories. Close and similar separations are noted for those positions endo to the bent molecular framework and hydride bridge. Intermediate distances separate those sites that are roughly in front and in back of the hydride bridge. The largest separations are found for those coordination sites that are over the top of the bridge or exo to the molecular framework bend. According to this approach then it is reasonable that the larger bridging ligand, Ph₂P(CH₂)₄PPh₂, spans the top of the bent molecular anion taking up coordination sites 2 and 9 according to our model and leaves the remaining coordination sites relatively unperturbed (Table IX). The expectation that the smaller bridging ligand should span the bottom or occupy the endo position is not realized, but rather "cis" positions are taken, and the other coordination site positions are drawn somewhat closer together. Such a substitution most

(20) Mague, J. T. *Inorg. Chem.* **1983**, *22*, 45 and references therein.

(21) Cowie, M.; Dwight, S. K. *Inorg. Chem.* **1980**, *19*, 2500.

(22) Cowie, M.; Dwight, S. K. *Inorg. Chem.* **1980**, *19*, 2508.

(23) Contact distances were calculated between corresponding C-O midpoints (which give values that agree well with the ca. 2.5 Å of a typical Mo-P distance) using the Enraf-Nonius SDP system of programs.

(19) Handy, L. B.; Ruff, J. K.; Dahl, L. F.; Hayter, R. G. *J. Am. Chem. Soc.* **1970**, *92*, 7312.

Table VIII. Comparison of Pertinent Distances (Å) and Angles (deg) for Binuclear Bridging Hydrides of Molybdenum

distances	[K(crypt)] ⁺	[PPN] ⁺	[Et ₄ N ⁺] (μ-H)Mo ₂ (CO) ₆ ⁻ PPh ₃ ^{-b}	[Et ₄ N ⁺] (μ-H)Mo ₂ (CO) ₆ ⁻ (PMePh ₂) ₂ ^{-c}	[Ph ₄ P ⁺] ¹⁻	[Et ₄ N ⁺] ⁴⁻
Mo ₁ -H	1.89 (4)	1.76 (5)	1.68 (5)	^c	1.89 (6)	1.92 (7)
Mo ₂ -H	1.91 (4)	1.93 (5)	2.19 (6)	^c	1.85 (6)	1.88 (7)
Mo...Mo	3.4056 (5)	3.4219 (9)	3.4736 (7)	3.443 (1)	3.4028 (8)	3.4995 (8)
Mo ₁ -P ₁				2.540 (4)	2.513 (2)	2.522 (2)
Mo ₂ -P ₂			2.565 (1)	2.543 (4)	2.509 (2)	2.556 (2)
angles						
Mo-H-Mo	127 (2)	136 (3)	127 (3)	^c	131 (3)	133 (3)
framework bend ^d	148	166	163	148	161	158
twist or staggering ^e	45	45	24	43	22	42

^a Reference 5. ^b Reference 7. ^c Reference 8. The hydride was not located in this structure. ^d This is defined as the angle of intersection of the two Mo-(CO)_{ax} vectors. Discussion in text. ^e This is defined as the angle between appropriate pairs of planes containing the axial CO, the Mo atom, and the equatorial CO or P atom on each coordination center.

Table IX. Coordination Site Position Separations^a

sites	anion		
	(μ-H)Mo ₂ (CO) ₁₀ ⁻	1 ⁻	4 ⁻
endo			
4...6	3.26		
4...7	3.28	3.06	3.25
1...7	3.33		
"cis"			
3...6	3.67	(3.19) ^b	3.95
1...8	3.79	3.64	4.07
exo			
2...8	4.22		
3...9	4.55		
2...9	6.65	4.65	(5.08) ^c

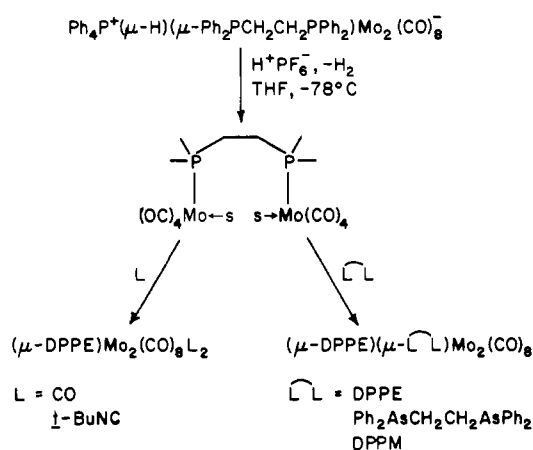
^a Calculated for points 2.5 Å along the Mo-CO vectors as discussed in text and referenced to Figure 7. See ref 23. ^b The P...P distance of 1⁻. ^c The P...P distance of 4⁻.

likely minimizes steric hindrance between the ligand phenyl groups and the CO ligands.

We had hoped that the requirements of the DPM ligand might have prompted the formation of the first example of a bent, eclipsed structure in the (μ-H)M₂L₁₀⁻ family of anions. Note, however, that an eclipse of the two coordination spheres at the same framework bend angle would position the endo coordination sites, 4...7, at < 3.06 Å and would probably invoke severe steric repulsions of the two CO oxygens of 4 and 7. More promising was the prediction that the other two cis coordination sites, 1...8, were just as available for DPM coordination as were the original 3...6 sites. In fact, the photochemical synthesis of (μ-H)(μ-DPM)₂Mo₂(CO)₆⁻ has been successful and will be reported separately.

Reactions of the (μ-H)(μ-P)Mo₂(CO)₈⁻ Anions with Acids. The initial goal of these studies was to determine whether the diphos or diphos-type bridge could survive the removal of the hydride bridge. Most of the acidification reactions were carried out with use of the less expensive bis(diphenylphosphino)ethane, Ph₂PCH₂CH₂PPh₂, or DPPE, derivative or 2⁻ as its Ph₄P⁺ salt. As illustrated in Scheme I, protonation presumably produces H₂ gas and an intermediate with two "open" coordination sites. Both the monodentate ligands CO and *t*-BuNC as well as the bidentate ligands Ph₂P(CH₂)_nPPh₂, *n* = 1, 2, and Ph₂AsCH₂CH₂AsPh₂ serve to capture the solvent stabilized coordinatively unsaturated intermediate as indicated in Scheme I. When acidified in CH₃CN the stability of the Mo-P bonds of the bridge in the intermediate is evident in that the decomposition mode of the complex dimer, in the absence of added ligand, is that of degradative loss of CO by some of the intermediates and its capture by others, ultimately producing (in low yield) the same dimer, (OC)₅Mo-DPPE-Mo(CO)₅,^{24,25} which is obtained on addition of CO during low-

Scheme I



temperature acidification. Similar diphos-bridged dimers have been prepared by Keiter, et al.,²⁶ via the base-catalyzed, ligand-linking reaction of (OC)₅MPPPh₂H and (OC)₅M'PPh₂CH=CH₂. Although the starting materials are more exotic than those reported here, the Keiter method has the advantage of providing a route to mixed-metal, phosphine-bridged dimers.

The acidification of the phosphine-bridged hydride anions in the presence of other bidentate ligands provides a convenient route to doubly bridged neutral bimetallics. It is not necessary that the bridges be identical. The resulting neutral dimers were identified by elemental analyses and infrared spectroscopy (Table III). Consistent with the ν(CO) IR pattern, their structures are expected to contain the bridging ligands in cis positions, yielding each metal in a local isolated C_{2v} or pseudo-C_{2v} environment.²⁷ The ligands and metals hence form large dimetallo-cycles somewhat like that of (OC)₄Cr-AsMe₂AsMe₂Cr(CO)₄AsMe₂AsMe₂, whose crystal structure was determined by Cotton and Webb.²⁸ Analogous complexes containing double bidentate ligand bridges have been prepared by others;^{29,30} however, the synthesis described above is superior for its capability of building specific mixed-bridged complexes.

Acknowledgment. Support for this work was provided by a grant from the donors of the Petroleum Research Fund (to M.Y.D.).

(25) J. A. Connor and G. A. Hudson, *J. Organomet. Chem.* **1974**, *73*, 351.

(26) Keiter, R. L.; Kaiser, S. L.; Hansen, N. P.; Brodack, J. W.; Cary, L. W. *Inorg. Chem.* **1981**, *20*, 283.

(27) The expected 4-band pattern is frequently overlapped (Darensbourg, M. Y.; Darensbourg, D. J. *J. Chem. Educ.* **1970**, *47*, 33). In this case the broad, strong band at ca. 1900 cm⁻¹ is a mixture of two degenerate vibrational modes.

(28) Cotton, F. A.; Webb, T. R. *Inorg. Chim. Acta* **1974**, *10*, 127.

(29) Beall, T. W.; Houk, L. W. *J. Organomet. Chem.* **1973**, *56*, 261 and references therein.

(30) Tripathi, S. C.; Srivastava, S. C.; Shrimal, A. K. *J. Organomet. Chem.* **1974**, *73*, 343 and references therein.

(24) Traces of Mo(CO)₄DPPE are obtained in this decomposition. Presumably the monomeric product would be more prominent (in accordance with eq 2) were the reaction run at temperatures more conducive to P-Mo and Mo-CO bond breaking.²⁵

administered by the American Chemical Society. Appreciation is expressed to Patricia Klahn-Coble for assistance with the NMR measurements, to Jeffrey Petersen for helpful discussion, and to Robert R. Burch, Jr., who made the first compounds of this type.

Registry No. 1⁻Et₄N⁺, 89231-95-8; 1⁻Ph₄P⁺, 89232-02-0; 2⁻Et₄N⁺, 89231-97-0; 2⁻Ph₄P⁺, 89232-03-1; 3⁻Et₄N⁺, 89231-99-2; 4⁻Et₄N⁺, 89232-01-9; 4⁻Ph₄P⁺, 89255-66-3; (μ-Ph₂PCH₂PPh₂)(μ-Ph₂P(CH₂)₂PPh₂)Mo₂(CO)₈, 89232-04-2; (μ-Ph₂P(CH₂)₂PPh₂)₂Mo₂(CO)₈, 89232-05-3; (μ-Ph₂P(CH₂)₂PPh₂)(μ-Ph₂As(CH₂)₂AsPh₂)Mo₂(CO)₈,

89232-06-4; (μ-Ph₂P(CH₂)₂PPh₂)[Mo(CO)₄(C≡N)C(CH₃)₃]₂, 89232-07-5; Et₄N⁺μ-HMo₂(CO)₁₀⁻, 12082-98-3; Ph₄P⁺μ-HMo₂(CO)₁₀⁻, 89255-65-2; H⁺PF₆⁻, 16940-81-1; CF₃COOH, 76-05-1.

Supplementary Material Available: Comprehensive listings of bond lengths and angles for Ph₄P⁺1⁻, Table S1, and Et₄N⁺4⁻, Table S2; observed and calculated structure factors, Tables S3 and S4; and anisotropic thermal parameters, Tables S5 and S6, for both structures (34 pages). Ordering information is given on any current masthead page.

Partial Electron Delocalization in a Mixed-Valence Trinuclear Iron(III)–Iron(II) Complex¹

Roderick D. Cannon,*^{2a} Ladda Montri,^{2a} David B. Brown,^{2b,c} Kerry M. Marshall,^{2b} and C. Michael Elliott^{2d}

Contribution from the School of Chemical Sciences, University of East Anglia, Norwich NR4 7TJ, England, Department of Chemistry, University of Vermont, Burlington, Vermont 05405, and Department of Chemistry, Colorado State University, Fort Collins, Colorado 80523. Received June 15, 1983

Abstract: Mixed-valence tri-μ-oxo iron acetates, [Fe^{III}₂Fe^{II}O(OOCCH₃)₆L₃], L = H₂O or pyridine, are considered from the standpoint of their intramolecular electron transfer rates. Data from Mössbauer and infrared spectra and solution redox chemistry indicate that these complexes are in the Robin and Day class II, but with appreciable electron delocalization. Adiabatic potential energy surfaces are calculated for the three-center mixed-valence case and fitted to the physical data available for the mixed-valence iron trimers.

Although a great many mixed-valence compounds have been examined, it has been possible to get direct information on the dynamics of the intramolecular electron transfer process in only a few cases.³⁻⁵ Of particular interest are the tri-μ-oxo iron acetates [Fe^{III}₂Fe^{II}O(OOCCH₃)₆L₃], L = H₂O or pyridine. At low temperatures, the Mössbauer spectra^{4,6} of these complexes reveal the existence of discrete Fe(III) and Fe(II) states, in the expected 2:1 ratio, thereby establishing valence trapping, or Robin and Day class II behavior.⁷ At higher temperatures, a single Mössbauer absorption is seen, suggesting that the valencies have become equivalent by an electron transfer process, eq 1, i.e., Robin and



Day class III behavior. There are two ways in which such equivalence can occur, one apparent and one real. The first is simply that the rate constant k_{et} has increased according to the Arrhenius law, eq 2, to the point where the rate is fast compared

$$k_{\text{et}} = \nu_0 \exp(-E_a/RT) \quad (2)$$

to the time frame of the experimental technique ($\approx 10^{-8}$ s in the case of the Mössbauer experiment). The second is that the molecular structure changes with temperature until the sites become structurally identical. In such a case the valencies are equivalent with respect to any experimental probe that has a time frame longer than that of a purely electronic transition ($\approx 10^{-14}$ s).

The Mossbauer data suggest that in the present complexes the latter type of transition does occur. The model used to fit the spectra as a function of temperature leaves not only the electron transfer relaxation time but also the isomer shifts and quadrupole splittings as adjustable parameters. As the temperature is increased, the isomer shifts and quadrupole splittings for Fe(III) and Fe(II) sites converge on each other. For the aquo complex, rough extrapolation suggests that they will converge between 300 and 350 K. For the pyridine complex the data are of poorer quality, but comparison with the aquo complex suggests that the convergence will be at a lower temperature.

Infrared data however indicate that the mixed-valence complexes are intermediate between localized and delocalized descriptions at lower temperatures as well. For a class III delocalized formulation the symmetry would be D_{3h} and the vibrational spectrum would be expected to correlate band for band with those of the fully oxidized complexes, [Fe^{III}₃O(OOCCH₃)₆L₃]⁺. For a class II localized formulation the symmetry would be lowered to C_{2v} and the spectrum would correlate with those of mixed-metal complexes [M₂M'O(OOCCH₃)₆L₃]⁺⁺. In the metal-carboxylate stretching region, the expected symmetry lowering was searched for but not found.^{8b} Although the bands were broad and might therefore conceal some small splittings, the result suggested that in the mixed-valence complexes the difference between Fe(III) and Fe(II) is at least partly suppressed. More recent data provide clearer support for this. In the symmetrical Fe^{III}₃O complexes, the doubly degenerate asymmetric Fe₃O stretch has been identified^{8a,9} (see Figure 1 and caption). In the mixed-metal series Fe^{III}₂M'O, M' = Mn, Co, Ni, the degeneracy of this mode is lifted and a doublet is seen. In the mixed-valence Fe^{III}₂Fe^{II}O complexes the doublet is detectable, but in comparison with the mixed-metal complexes (and particularly in the pyridine series) the splitting is less and the component bands are broader and less intense.

(1) Presented in part at the Conference on Inorganic Reaction Mechanisms, Wayne State University, Detroit, MI, June 1981.

(2) (a) East Anglia; (b) Vermont; (c) deceased; (d) Colorado.

(3) Gagné, R. R.; Koval, C. A.; Smith, T. J.; Cimolino, M. C. *J. Am. Chem. Soc.* **1979**, *101*, 4571.

(4) Dziobkowski, C. T.; Wroblewski, J. T.; Brown, D. B. *Inorg. Chem.* **1981**, *20*, 679.

(5) Sanchez, C.; Livage, J.; Launay, J. P.; Fournier, M.; Jeannin, J. *J. Am. Chem. Soc.* **1982**, *104*, 3194.

(6) Lupu, D.; Barb, D.; Filoti, G.; Morariu, M.; Tarnia, D. *J. Inorg. Nucl. Chem.* **1972**, *34*, 2803.

(7) Robin, M. B.; Day, P. *Adv. Inorg. Chem. Radiochem.* **1967**, *10*, 247.

(8) (a) Johnson, M. K.; Powell, D. B.; Cannon, R. D. *Spectrochim. Acta, Part A* **1981**, *37A*, 995; (b) *Ibid.* **1982**, *38A*, 307.

(9) Montri, L.; Cannon, R. D.; in preparation.